CRYSTALLOGRAPHIC COMMUNICATIONS

ISSN 2056-9890

Formamidinium iodide: crystal structure and phase transitions

Andrey A. Petrov,[a] Eugene A. Goodilin,[a,b] Alexey B. Tarasov,[a,b]* Vladimir A. Lazarenko,[c] Pavel V. Dorovatovskii[c] and Victor N. Khrustalev[d,e]

[a]Department of Materials Science, Lomonosov Moscow State University, Lenin Hills, 119991 Moscow, Russian Federation, [b]Department of Chemistry, Lomonosov Moscow State University, Lenin Hills, 119991 Moscow, Russian Federation, [c]National Research Centre 'Kurchatov Institute', 1 Acad. Kurchatov Sq., Moscow 123182, Russian Federation, [d]Inorganic Chemistry Department, Peoples' Friendship University of Russia (RUDN University), 6 Miklukho-Maklay St., Moscow 117198, Russian Federation, and [e]X-Ray Structural Centre, A. N. Nesmeyanov Institute of Organoelement Compounds, Russian Academy of Sciences, 28 Vavilov St., B-334, Moscow 119991, Russian Federation. *Correspondence e-mail: alexey.bor.tarasov@gmail.com

Received 9 March 2017
Accepted 16 March 2017

Edited by A. J. Lough, University of Toronto, Canada

Keywords: crystal structure; formamidinium iodide; phase transitions; powder diffraction; synchrotron radiation.

CCDC reference: 1538402

Supporting information: this article has supporting information at journals.iucr.org/e

At a temperature of 100 K, $CH_5N_2^+\cdot I^-$ (**I**), crystallizes in the monoclinic space group $P2_1/c$. The formamidinium cation adopts a planar symmetrical structure [the r.m.s. deviation is 0.002 Å, and the C—N bond lengths are 1.301 (7) and 1.309 (8) Å]. The iodide anion does not lie within the cation plane, but deviates from it by 0.643 (10) Å. The cation and anion of **I** form a tight ionic pair by a strong N—H···I hydrogen bond. In the crystal of **I**, the tight ionic pairs form hydrogen-bonded zigzag-like chains propagating toward [20$\bar{1}$] *via* strong N—H···I hydrogen bonds. The hydrogen-bonded chains are further packed in stacks along [100]. The thermal behaviour of **I** was studied by different physicochemical methods (thermogravimetry, differential scanning calorimetry and powder diffraction). Differential scanning calorimetry revealed three narrow endothermic peaks at 346, 387 and 525 K, and one broad endothermic peak at ~605 K. The first and second peaks are related to solid–solid phase transitions, while the third and fourth peaks are attributed to the melting and decomposition of **I**. The enthalpies of the phase transitions at 346 and 387 K are estimated as 2.60 and 2.75 kJ mol^{-1}, respectively. The X-ray powder diffraction data collected at different temperatures indicate the existence of **I** as the monoclinic (100–346 K), orthorhombic (346–387 K) and cubic (387–525 K) polymorphic modifications.

1. Chemical context

Compounds with the general formula ABX_3 [where A denotes an organic cation *e.g.* methylammonium (MA, $CH_3NH_3^+$) or formamidinium [FA = $CH(NH_2)_2$, CH_3NH_3]; B = Pb, Sn; X = I, Br, Cl] belong to a class of hybrid organic–inorganic perovskites and perform as outstanding light harvesters. These compounds gave birth to a new field of photovoltaics – perovskite solar cells – when Kojima and co-authors used $(MA)PbI_3$ as a light sensitizer for the first time in dye-sensitized solar cells (DSSCs) in 2009 and showed 3.8% efficiency (Kojima *et al.*, 2009). Since then, a revolutionary breakthrough has occured in this area and the highest efficiency now has reached 22.1%.

In 2014, the formamidinium cation was proposed to replace methylammonium and the further investigation of $(FA)PbI_3$ disclosed its superiority to $(MA)PbI_3$ (Koh *et al.*, 2014; Pang *et al.*, 2014). In particular, it was found that $(FA)PbI_3$ exhibits higher thermal and moisture stability and has a lower bandgap than $(MA)PbI_3$ which gives a greater capacity for sunlight absorption (Koh *et al.*, 2014; Han *et al.*, 2016). Recently, it was

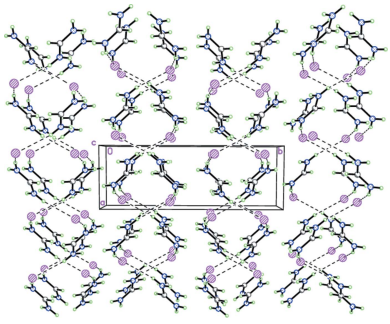

shown that the properties of the compounds may be further optimized by tuning the MA/FA ratio and an efficiency of 20.5% has been reached for a mixed compound (Li *et al.*, 2016; Jeon *et al.*, 2015).

The main precursors to obtain $(FA)PbI_3$ are PbI_2 and formamidinium iodide (FA)I. Several methods of perovskite synthesis include steps where it can be obtained directly from (FA)I in a crystalline form (Zhou *et al.*, 2015; Leyden *et al.*, 2015). It also appears in a crystalline form and leads to a formation of low-dimensional phases when an excess of it is taken (Xi *et al.*, 2016; Ma *et al.*, 2017). Thus, the understanding of the (FA)I crystal structure gives valuable information for understanding the crystallization of formamidinium-based lead halide perovskites. Knowledge of the (FA)I crystal structure may also be of particular interest for computer simulations of the processes related to the crystallization of these perovskites. Surprisingly, despite the hundreds of papers published over the last several years that have mentioned (FA)I as a major precursor for hybrid lead halide perovskites, its crystal structure has remained unknown so far.

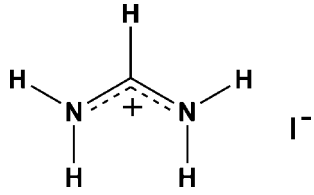

In this work, we investigated the structure of (FA)I (**I**) and its thermal behaviour by different physico-chemical methods.

2. Structural commentary

At a temperature of 100 K, compound **I** crystallizes in the monoclinic space group $P2_1/c$. The formamidinium cation adopts a planar symmetrical structure [r.m.s. deviation is 0.002 Å, and the C—N bond lengths are 1.301 (7) and 1.309 (8) Å; Fig. 1]. The iodide anion does not lie within the cation plane, but deviates from it by 0.643 (10) Å. The cation and anion in **I** form a tight ionic pair by the strong N1—H1*A*···I1 hydrogen bond (Table 1 and Fig. 1).

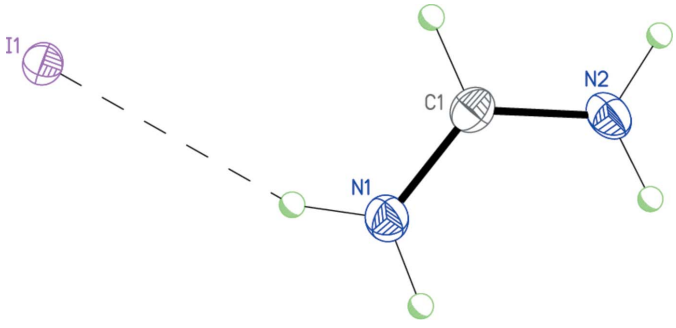

Figure 1
The molecular structure of salt **I**. Displacement ellipsoids are shown at the 50% probability level. H atoms are presented as small spheres of arbitrary radius. Dashed line indicates the intermolecular N—H···I hydrogen bond.

Table 1
Hydrogen-bond geometry (Å, °).

D—H···*A*	*D*—H	H···*A*	*D*···*A*	*D*—H···*A*
N1—H1*A*···I1	0.90	2.77	3.612 (5)	156
N2—H2*A*···I1^{i}	0.90	2.74	3.622 (4)	166

Symmetry code: (i) $x-1, -y+\frac{1}{2}, z+\frac{1}{2}$.

In order to understand the thermal behaviour of **I** at elevated temperatures, the sample was investigated by TG and DSC methods in the temperature region from 293 to 750 K at a rate of 5 K min^{-1}. The mass loss started from ∼520 K (Fig. 2). Differential scanning calorimetry revealed three narrow endothermic peaks at 346, 387 and 525 K, and one broad endothermic peak at ∼605 K. The first and the second peaks are related to solid–solid phase transitions, while the third and the fourth peaks are attributed to the melting and decomposition of **I**. Enthalpy of the phase transitions at 346 and 387 K are estimated as 2.24 and 2.87 kJ mol^{-1}, respectively.

The X-ray powder diffraction data collected at different temperatures confirm the existence of different phases (Fig. 3). At low temperatures, salt **I** exists in a monoclinic phase and exhibits a significant change of the parameters with a rise in temperature (100 → 195 → 293 K, Fig. 3). A phase existing at 358 K is indexed in an orthorhombic crystal system [a = 7.3915 (8) Å, b = 6.3358 (8) Å, c = 5.2391 (9) Å; $M(20)$ = 25, $F(20)$ = 45]. Another high-temperature phase is cubic, exhibiting only a few reflections at 400 K [a = 5.0571 (5) Å; $M(13)$ = 126, $F(13)$ = 109]. It seems to be a plastic phase similar to a plastic phase for methylammonium iodide (Ishida *et al.*, 1995; Yamamuro *et al.*, 1992).

3. Supramolecular features

In the crystal of **I**, the tight ionic pairs form hydrogen-bonded zigzag-like chains propagating toward [20$\bar{1}$] by the strong intermolecular N2—H2*A*···I1^{i} hydrogen bonds (Table 1 and Fig. 4). The hydrogen-bonded chains are further packed in

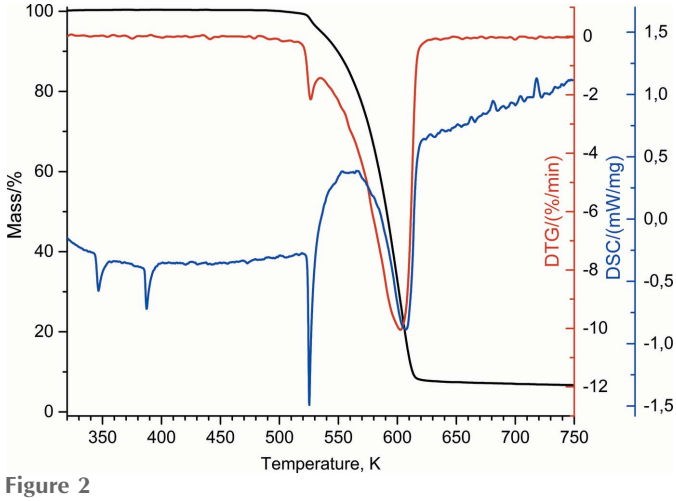

Figure 2
Thermogravimetry and differential scanning calorimetry analyses for **I**.

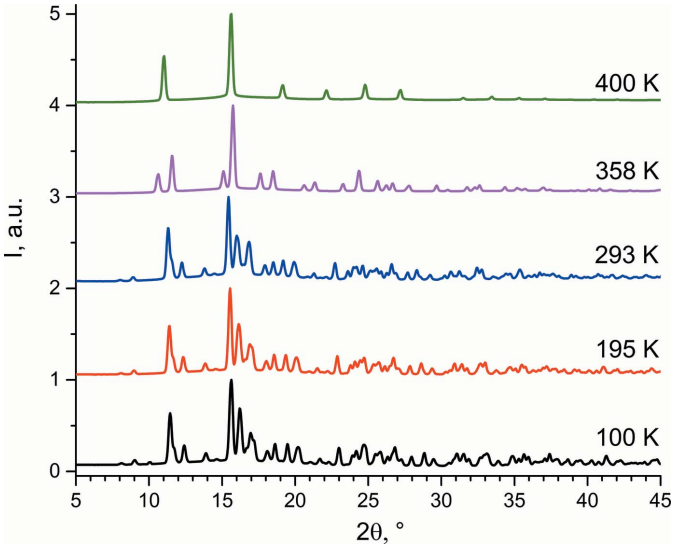

Figure 3
X-ray powder diffraction data for **I** at different temperatures.

stacks along [100] (Fig. 4) [symmetry code: (i) $x-1, -y+\frac{1}{2}, z+\frac{1}{2}$].

4. Synthesis and crystallization

Polycrystalline powder of **I** was purchased from Dyesol and used without further purification. Single crystals suitable for X-ray structural study were obtained by recrystallization from an anhydrous ethanol solution by slow cooling.

5. Refinement

Crystal data, data collection and structure refinement details are summarized in Table 2. X-ray diffraction study of **I** was carried out on the 'Belok' beamline of the National Research Center 'Kurchatov Institute' (Moscow, Russian Federation) using a Rayonix SX165 CCD detector. Reflection intensities measured were corrected for absorption using the *Scala* (Evans, 2006) program.

The H atoms of the NH_2 groups were localized in the difference Fourier map and refined with fixed positional and isotropic displacement parameters [U_{iso}(H) = 1.2U_{eq}(N)]. The CH hydrogen was placed in a calculated position, with C—H = 0.95 Å, and refined in the riding model with a fixed isotropic displacement parameter [U_{iso}(H) = 1.2U_{eq}(C)].

Table 2
Experimental details.

Crystal data	
Chemical formula	$CH_5N_2^+\cdot I^-$
M_r	171.97
Crystal system, space group	Monoclinic, $P2_1/c$
Temperature (K)	100
a, b, c (Å)	4.8211 (6), 13.776 (3), 7.0113 (10)
β (°)	98.06 (3)
V (Å^3)	461.06 (14)
Z	4
Radiation type	Synchrotron, λ = 0.96990 Å
μ (mm^{-1})	15.38
Crystal size (mm)	0.06 × 0.05 × 0.03
Data collection	
Diffractometer	Rayonix SX165 CCD
Absorption correction	Multi-scan (*SCALA*; Evans, 2006)
T_{min}, T_{max}	0.400, 0.600
No. of measured, independent and observed [$I > 2\sigma(I)$] reflections	5111, 949, 894
R_{int}	0.070
(sin $\theta/\lambda)_{max}$ (Å^{-1})	0.642
Refinement	
$R[F^2 > 2\sigma(F^2)]$, $wR(F^2)$, S	0.039, 0.093, 1.06
No. of reflections	949
No. of parameters	38
H-atom treatment	H-atom parameters constrained
$\Delta\rho_{max}$, $\Delta\rho_{min}$ (e Å^{-3})	0.87, −0.91

Computer programs: *Marccd* (Doyle, 2011), *iMosflm* (Battye *et al.*, 2011), *SHELXT* (Sheldrick, 2015*a*), *SHELXL2014* (Sheldrick, 2015*b*) and *SHELXTL* (Sheldrick, 2008).

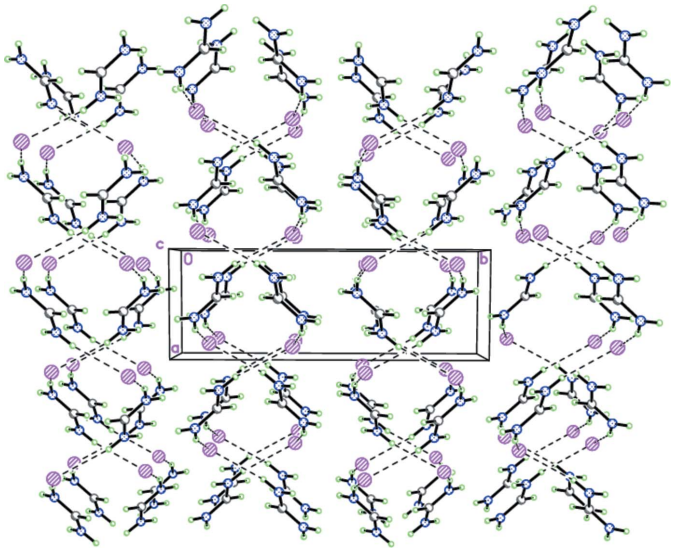

Figure 4
The crystal structure of **I** demonstrating the hydrogen-bonded zigzag-like chains propagating toward [20$\bar{1}$]. Dashed lines indicate the intermolecular N—H···I hydrogen bonds.

Acknowledgements

This work was supported financially by the Ministry of Education and Science of the Russian Federation (the Agreement number 02.a03.21.0008). AT, AP and EG acknowledge the Russian Foundation for Basic Research for funding the reported study as part of research project No. 16-29-03291.

References

Battye, T. G. G., Kontogiannis, L., Johnson, O., Powell, H. R. & Leslie, A. G. W. (2011). *Acta Cryst.* D**67**, 271–281.
Doyle, R. A. (2011). *Marccd software manual*. Rayonix L. L. C., Evanston, IL 60201, USA.
Evans, P. (2006). *Acta Cryst.* D**62**, 72–82.
Han, Q., Bae, S.-H., Sun, P., Hsieh, Y.-T., Yang, Y. M., Rim, Y. S., Zhao, H., Chen, Q., Shi, W., Li, G. & Yang, Y. (2016). *Adv. Mater.* **28**, 2253–2258.

Ishida, H., Maeda, H., Hirano, A., Fujimoto, T., Kubozono, Y., Kashino, S. & Emura, S. (1995). *Z. Naturforsch. Teil A*, **50**, 14–18.
Jeon, N. J., Noh, J. H., Yang, W. S., Kim, Y. C., Ryu, S., Seo, J. & Seok, S. I. (2015). *Nature*, **517**, 476–480.
Koh, T. M., Fu, K., Fang, Y., Chen, S., Sum, T. C., Mathews, N., Mhaisalkar, S. G., Boix, P. P. & Baikie, T. (2014). *J. Phys. Chem. C*, **118**, 16458–16462.
Kojima, A., Teshima, K., Shirai, Y. & Miyasaka, T. (2009). *J. Am. Chem. Soc.* **131**, 6050–6051.
Leyden, M. R., Lee, M. V., Raga, S. R. & Qi, Y. (2015). *J. Mater. Chem.* A**3**, 16097–16103.
Li, X., Bi, D., Yi, C., Decoppet, J.-D., Luo, J., Zakeeruddin, S. M., Hagfeldt, A. & Gratzel, M. (2016). *Science*, **353**, 58–62.
Ma, F., Li, J., Li, W., Lin, N., Wang, L. & Qiao, J. (2017). *Chem. Sci.* **8**, 800–805.
Pang, S., Hu, H., Zhang, J., Lv, S., Yu, Y., Wei, F., Qin, T., Xu, H., Liu, Z. & Cui, G. (2014). *Chem. Mater.* **26**, 1485–1491.
Sheldrick, G. M. (2008). *Acta Cryst.* A**64**, 112–122.
Sheldrick, G. M. (2015*a*). *Acta Cryst.* A**71**, 3–8.
Sheldrick, G. M. (2015*b*). *Acta Cryst.* C**71**, 3–8.
Xi, J., Wu, Z., Xi, K., Dong, H., Xia, B., Lei, T., Yuan, F., Wu, W., Jiao, B. & Hou, X. (2016). *Nano Energy*, **26**, 438–445.
Yamamuro, O., Matsuo, T., Suga, H., David, W. I. F., Ibberson, R. M. & Leadbetter, A. J. (1992). *Acta Cryst.* B**48**, 329–336.
Zhou, Y., Yang, M., Vasiliev, A. L., Garces, H. F., Zhao, Y., Wang, D., Pang, S., Zhu, K. & Padture, N. P. (2015). *J. Mater. Chem. A*, **3**, 9249–9256.

supporting information

Acta Cryst. (2017). E**73**, 569-572 [https://doi.org/10.1107/S205698901700425X]

Formamidinium iodide: crystal structure and phase transitions

Andrey A. Petrov, Eugene A. Goodilin, Alexey B. Tarasov, Vladimir A. Lazarenko, Pavel V. Dorovatovskii and Victor N. Khrustalev

Computing details

Data collection: Marccd (Doyle, 2011); cell refinement: iMosflm (Battye *et al.*, 2011); data reduction: iMosflm (Battye *et al.*, 2011); program(s) used to solve structure: SHELXT (Sheldrick, 2015a); program(s) used to refine structure: *SHELXL2014* (Sheldrick, 2015b); molecular graphics: *SHELXTL* (Sheldrick, 2008); software used to prepare material for publication: *SHELXTL* (Sheldrick, 2008).

Formamidinium iodide

Crystal data

$CH_5N_2^+ \cdot I^-$
M_r = 171.97
Monoclinic, $P2_1/c$
a = 4.8211 (6) Å
b = 13.776 (3) Å
c = 7.0113 (10) Å
β = 98.06 (3)°
V = 461.06 (14) Å^3
Z = 4
$F(000)$ = 312
D_x = 2.477 Mg m^{-3}
Synchrotron radiation, λ = 0.96990 Å
Cell parameters from 600 reflections
θ = 4.0–36.0°
μ = 15.38 mm^{-1}
T = 100 K
Prism, colourless
0.06 × 0.05 × 0.03 mm

Data collection

Rayonix SX165 CCD diffractometer
φ scan
Absorption correction: multi-scan (Scala; Evans, 2006)
T_{min} = 0.400, T_{max} = 0.600
5111 measured reflections
949 independent reflections
894 reflections with $I > 2\sigma(I)$
R_{int} = 0.070
θ_{max} = 38.5°, θ_{min} = 4.0°
h = −6→6
k = −17→17
l = −8→7

Refinement

Refinement on F^2
Least-squares matrix: full
$R[F^2 > 2\sigma(F^2)]$ = 0.039
$wR(F^2)$ = 0.093
S = 1.06
949 reflections
38 parameters
0 restraints
Primary atom site location: difference Fourier map
Secondary atom site location: difference Fourier map
Hydrogen site location: mixed
H-atom parameters constrained
$w = 1/[\sigma^2(F_o^2) + 0.7865P]$ where $P = (F_o^2 + 2F_c^2)/3$
$(\Delta/\sigma)_{max} < 0.001$
$\Delta\rho_{max}$ = 0.87 e Å^{-3}
$\Delta\rho_{min}$ = −0.91 e Å^{-3}
Extinction correction: SHELXL2014 (Sheldrick, 2015b), $Fc^* = kFc[1+0.001xFc^2\lambda^3/\sin(2\theta)]^{-1/4}$
Extinction coefficient: 0.0064 (11)

Special details

Geometry. All esds (except the esd in the dihedral angle between two l.s. planes) are estimated using the full covariance matrix. The cell esds are taken into account individually in the estimation of esds in distances, angles and torsion angles; correlations between esds in cell parameters are only used when they are defined by crystal symmetry. An approximate (isotropic) treatment of cell esds is used for estimating esds involving l.s. planes.

Fractional atomic coordinates and isotropic or equivalent isotropic displacement parameters (Å²)

	x	*y*	*z*	U_{iso}*/U_{eq}
I1	0.86658 (6)	0.38577 (2)	0.20022 (5)	0.0218 (2)
N1	0.6120 (9)	0.4171 (3)	0.6569 (7)	0.0250 (10)
H1A	0.7250	0.4174	0.5650	0.030*
H1B	0.6251	0.4648	0.7454	0.030*
N2	0.2540 (9)	0.3389 (3)	0.7860 (7)	0.0254 (11)
H2A	0.1352	0.2882	0.7776	0.030*
H2B	0.2515	0.3832	0.8801	0.030*
C1	0.4296 (11)	0.3478 (4)	0.6606 (8)	0.0227 (11)
H1	0.4233	0.2994	0.5637	0.027*

Atomic displacement parameters (Å²)

	U^{11}	U^{22}	U^{33}	U^{12}	U^{13}	U^{23}
I1	0.0230 (3)	0.0215 (3)	0.0217 (4)	0.00012 (9)	0.0054 (2)	−0.00041 (10)
N1	0.022 (2)	0.030 (2)	0.023 (3)	−0.0030 (18)	0.0030 (19)	0.000 (2)
N2	0.021 (2)	0.022 (2)	0.034 (3)	−0.0020 (17)	0.008 (2)	0.0011 (19)
C1	0.023 (2)	0.026 (3)	0.019 (3)	0.002 (2)	0.001 (2)	0.000 (2)

Geometric parameters (Å, º)

N1—C1	1.301 (7)	N2—H2A	0.8999
N1—H1A	0.9001	N2—H2B	0.9000
N1—H1B	0.9001	C1—H1	0.9500
N2—C1	1.309 (8)		
C1—N1—H1A	119.7	H2A—N2—H2B	120.0
C1—N1—H1B	120.3	N1—C1—N2	125.8 (5)
H1A—N1—H1B	120.0	N1—C1—H1	117.1
C1—N2—H2A	119.7	N2—C1—H1	117.1
C1—N2—H2B	120.3		

Hydrogen-bond geometry (Å, º)

D—H···*A*	*D*—H	H···*A*	*D*···*A*	*D*—H···*A*
N1—H1*A*···I1	0.90	2.77	3.612 (5)	156
N2—H2*A*···I1^{i}	0.90	2.74	3.622 (4)	166

Symmetry code: (i) *x*−1, −*y*+1/2, *z*+1/2.